Quantum chaos in billiards

Arnd Bäcker

Institut für Theoretische Physik, Technische Universität Dresden, D-01062 Dresden, Germany

Abstract

Billiards are an important class of systems showing a large variety of dynamical behaviour ranging from integrable (i.e. regular) motion, over mixed dynamics to strongly chaotic behaviour. Using tools developed with Python one can interactively study the complexity of the dynamics. This dynamical behaviour is directly reflected in properties of the corresponding quantum systems, like eigenvalue statistics or the structure of eigenfunctions.

Chaotic behaviour in dynamical systems is a well-studied phenomenon. A particularly illustrative class of systems are so-called billiard systems where a point particle moves freely along straight lines inside a two-dimensional domain Ω with elastic reflections at the boundary. In such systems it is therefore exclusively the boundary which determines the dynamical properties. This is illustrated in Fig. 1 where 50 iterations of one initial point are shown for two billiards, parametrized in polar coordinates by $\rho(\varphi) = 1 + \varepsilon\cos(\varphi)$ with $\varphi \in [0, 2\pi]$, for parameters $\varepsilon = 0$ (circular billiard) and $\varepsilon = 1$ (cardioid billiard) [1]. The circular billiard is an example of an integrable system showing regular dynamics. The opposite extreme is the cardioid billiard which is fully chaotic In particular this means that nearby trajectories separate exponentially as a function of time (hyperbolicity) and that a typical trajectory will fill out the available space in a uniform way (ergodicity).

As the motion inside the billiard is on straight lines it is convenient to use the boundary to define a Poincaré section,

$$\mathcal{P} := \{(s, p) \mid s \in [0, |\partial\Omega|],\ p \in [-1, 1]\} \quad . \tag{1}$$

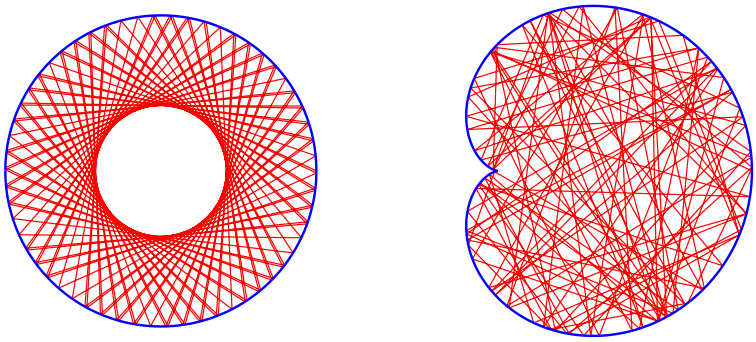

Figure 1: Regular dynamics in a billiard with circular shape vs. chaotic dynamics in the cardioid billiard.

Here s is the arclength along the boundary $\partial\Omega$ and $p = \langle \boldsymbol{v}, \boldsymbol{T}(s) \rangle$ is the projection of the unit velocity vector $\boldsymbol{v}$ after the reflection on the unit tangent vector $\boldsymbol{T}(s)$ in the point $s \in \partial\Omega$. The Poincaré map P of a point $\xi = (s, p) \in \mathcal{P}$ is then obtained by considering the ray starting at the point $\boldsymbol{r}(s) \in \partial\Omega$ in the direction specified by p and determining the first intersection with the boundary, leading to the new point $\xi' = (s', p')$. Explicitly, the velocity in the $\boldsymbol{T}, \boldsymbol{N}$ coordinate system is given by $(p, n = \sqrt{1-p^2})$, so that in Cartesian coordinates

$$\boldsymbol{v} = (v_x, v_y) = \begin{pmatrix} T_x & N_x \\ T_y & N_y \end{pmatrix} (p, n) = \left(T_x p + N_x \sqrt{1-p^2}, T_y p + N_y \sqrt{1-p^2} \right) \quad . \tag{2}$$

Numerically the main task is to find the next intersection for a given starting point on the boundary and direction, specified by s and p. If the boundary is determined by an implicit equation

$$F(x, y) = 0 \quad , \tag{3}$$

the new point $\boldsymbol{r}'$ can be determined by solving

$$F(x + t v_x, y + t v_y) = 0 \tag{4}$$

for $t > 0$. In the case of the circular billiard one easily obtains an analytical solution leading to an explicit prescription of the billiard mapping. In general, however, only a numerical solution of (4) is possible.

For non–convex billiards there are points $\xi = (s, p) \in \mathcal{P}$ for which there is more than one solution (apart from $t = 0$); obviously the one with the smallest $t > 0$ has to be chosen. The condition (3) can sometimes be used to remove the $t = 0$ solution analytically from (4). If F is a polynomial in x and y this allows to reduce the order of (4) by one. This approach has for

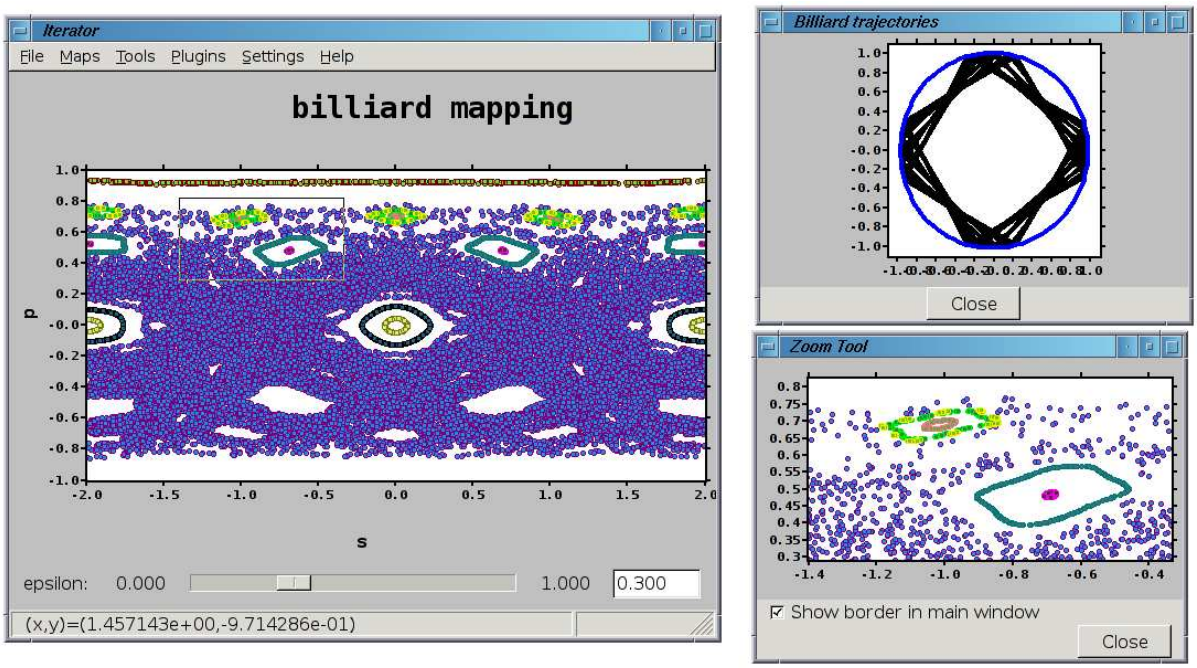

Figure 2: Screenshot of a Python application to interactively explore billiard systems.

example been used for the cardioid billiard leading to a cubic equation for t, see [2] for details. From the solution t one gets the coordinates $(x', y') = (x, y) + t\boldsymbol{v}$.

Numerically, one has to find one or several solutions of (4), depending on the type of boundary. Therefore one typically tries to bracket the zero with the smallest t, e.g. by evaluating $F(x+tv_x, y+tv_y)$ for sufficiently many values of t, and then use `scipy.optimize.brentq` to determine the zero as precisely as possible. Special attentention has to be given to glancing motion, e.g. when p is near ± 1 because then t can get very close to 0, or in non-convex billiards, zeros of $F(x+tv_x, y+tv_y)$ can become very close to each otherand can therefore be easily missed.

Both for research and teaching it proved extremely useful to interactively explore the dynamics in billiards using the visualization of trajectories specified by their initial condition in the Poincaré section using the mouse. For this purpose we developed an application written in Python, using `wxPython` [3] for the graphical user-interface and for fast plotting of many points a particular canvas [4]. Fig. 2 shows a typical screenshot, where the above billiard family is considered for $\varepsilon = 0.3$. In this case one has a system which shows both regular and irregular motion, depending on the initial point.

While classical mechanics describes macroscopic objects correctly, at small scales a quantum mechanical description is necessary. Due to the Heisenberg uncertainty principle it is no longer possible to specify both position and momentum of a particle at the same time. Instead the state of a particle is specified by a wave function whose absolute value squared is interpreted as the probability density. For quantum billiards finding the stationary solutions of the Schrödinger equation reduces to the determination of eigenvalues and eigenfunctions of the Helmholtz equation

$$-\Delta\psi_n(\boldsymbol{q}) = E_n\psi_n(\boldsymbol{q}) \quad , \quad \boldsymbol{q} \in \Omega \tag{5}$$

with (for example) Dirichlet boundary conditions, i.e. $\psi_n(\boldsymbol{q}) = 0$ for $\boldsymbol{q} \in \partial\Omega$. Here Δ denotes the Laplace operator, which reads in two dimensions $\Delta = \left(\frac{\partial^2}{\partial q_1^2} + \frac{\partial^2}{\partial q_2^2}\right)$. The interpretation of ψ is that $\int_D |\psi(\boldsymbol{q})|^2 \, \mathrm{d}^2q$ is the probability of finding the particle inside the domain $D \subset \Omega$.

For some simple domains Ω it is possible to solve eq. (5) analytically. For example for the billiard in a rectangle with sides a and b the (non–normalized) eigenfunctions are given by $\psi_{n_1,n_2}(\boldsymbol{q}) = \sin(\pi n_1 q_1/a)\sin(\pi n_2 q_2/b)$ with corresponding eigenvalues $E_{n_1,n_2} = \pi^2(n_1^2/a^2 + n_2^2/b^2)$ and $(n_1, n_2) \in \mathbb{N}^2$. For the billiard in a circle the eigenfunctions are given in polar–coordinates by $\psi_{mn}(r, \varphi) = J_m(j_{mn}r)\exp(\mathrm{i}m\varphi)$, where j_{mn} is the n–th zero of the Bessel function $J_m(x)$ and $m \in \mathbb{Z}$, $n \in \mathbb{N}$. Using `scipy.special.jn_zeros` one can easily obtain a given number of zeros of $J_m(x)$ for fixed m.

However, in general no analytical solutions of eq. (5) exist so that numerical methods have to be used to compute eigenvalues and eigenfunctions. Among the many different possibilities, the so-called boundary-integal method is widely used, see [5] for a more detailed account and references. By employing Green's theorem the two-dimensional problem (5) is transformed into a one-dimensional integral equation. Discretization leads to a matrix equation for which the zeros of a determinant as a function of the energy E have to be determined. To detect nearly degenerate energy levels it turned out to be most efficient [6] to use a singular value decomposition. Concerning the numerical implementation this is the most time consuming step, which is provided by `scipy.linalg.flapack.zgesdd`. Using this approach 2000-10000 (and more if necessary) eigenvalues and eigenfunctions can easily be computed. In particular, due to the independence of the computation at different E, this problem can be straight-forwardly parallelized using as many CPUs as available. Communication between different CPUs is essentially not needed, only the initial value of E has to transferred to each CPU (e.g. using MPI).

One of the fundamental questions in quantum chaos concerns the implications of the underylying classical dynamical properties on the statistical behaviour of eigenvalues. It has been conjectured that for fully chaotic systems these are described by the statics of random matrices obeying appropriate symmetries [7]. For generic integrable systems one expects that the energy level statistics can be described by a Poissonian random process [8].

The simplest spectral statistics is the level spacing distribution $P(s)$ obtained from the histogramm of the spacings

$$s_n := x_{n+1} - x_n \quad , \tag{6}$$

where x_n are rescaled eigenvalues such that their average spacing is 1. Once the eigenvalues are computed, the determination of the level-spacing distribution can be done as follows

```
from pylab import *

spacings = x[1:]-x[0:-1]                    # x: rescaled eigenvalues
hist(dat, normed=True, bins=100)
show()
```

The resulting distribution has to be compared with the expectation for integrable systems,

$$P_{\text{Poisson}}(s) = \mathrm{e}^{-s} \quad . \tag{7}$$

Since $P(s) \to 1$ for $s \to 0$ this behaviour is called *level attraction*. The result for the level-spacing distribution in the case of the Gaussian orthogonal random matrix ensemble (GOE) is in very good approximation described by the Wigner distribution [9]

$$P_{\text{GOE}}(s) \approx P_{\text{Wigner}}(s) = \frac{\pi}{2} s \exp\left(-\frac{\pi}{4} s^2\right) \quad . \tag{8}$$

In this case we have $P(s) \to 0$ for $s \to 0$, which is called *level repulsion*. To illustrate this behaviour, we show in fig. 3 the level-spacing distribution for the circle and for the cardioid billiard and observe good agreement with the expected distributions.

Concerning the eigenfunctions of (5) one would expect that the classical dynamics is reflected by their structure. According to the "semiclassical eigenfunction hypothesis" the eigenstates should concentrates on those regions which a generic orbit explores in the long–time limit [10–12].

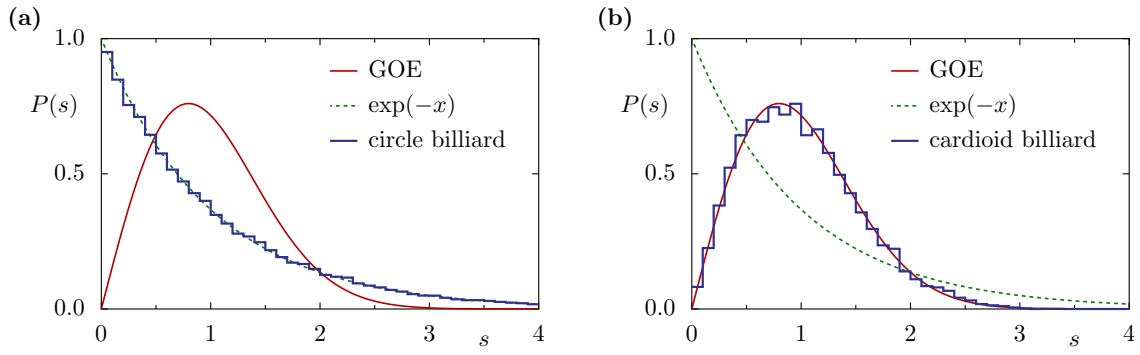

Figure 3: Level–spacing distribution for (a) circle billiard (100 000 eigenvalues) and (b) cardioid billiard (11 000 eigenvalues). On observes good agreement with the expected behaviour of a Poissonian random process and of the GOE, respectively

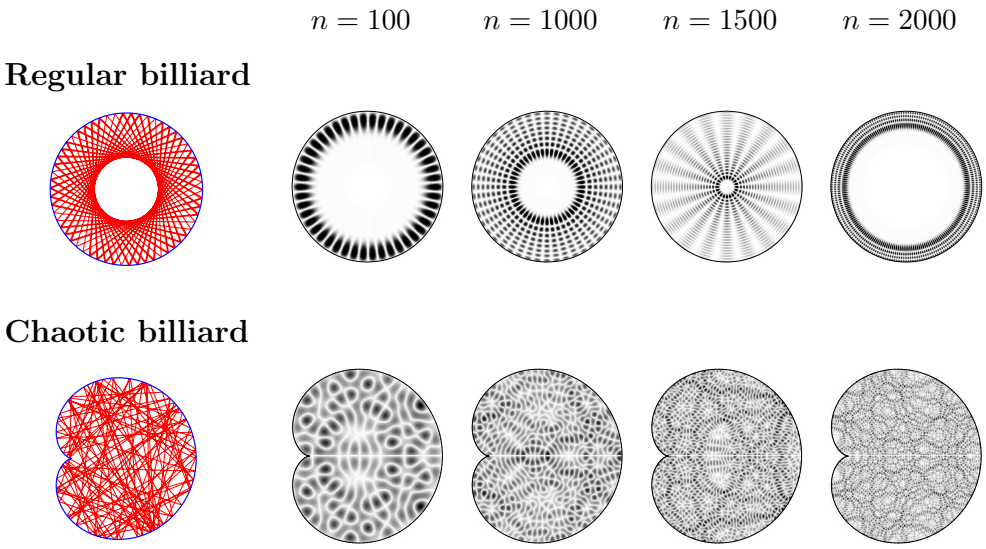

Figure 4: The eigenstates of the integrable circular billiard and the chaotic cardioid billiard reflect the structure of the corresponding classical dynamics.

For integrable systems the motion is restricted to invariant tori while for ergodic systems the whole energy surface is filled in a uniform way. For the case of ergodic systems this statement is actually proven by the quantum ergodicity theorem (see [13] for an introduction and references), which states that almost all eigenfunctions become equidistributed in the semiclassical limit, e.g. restricted to position space we have

$$\lim_{j\to\infty} \int_D |\psi_{n_j}(\boldsymbol{q})|^2 \, \mathrm{d}^2 q = \frac{\mathrm{vol}(D)}{\mathrm{vol}(\Omega)} \tag{9}$$

for a subsequence $\{\psi_{n_j}\} \subset \{\psi_n\}$ of density one. So for almost all eigenfunctions the probability of finding a particle in a certain region D of the position space Ω in the semiclassical limit is just the same as for the classical system.

Fig. 4 illustrates this for the case of the integrable circle billiard and the chaotic cardioid billiard. One clearly sees that in the former case the probability is restricted to subregions of the billiard, while for the ergodic case the probability density is uniformly distributed over the full billiard region (apart from the inevitable fluctuations).

For systems with a mixed phase space the dynamics is more complicated, because both regular motion and chaotic motion coexist, see Fig. 2. This is also reflected in the structure of the quantum eigenstates, which are either located in the regular islands, or extend over the chaotic region, see fig. 5

To conclude let us mention that in addition to the fundamental questions on the quantum behaviour of systems with classically chaotic dynamics, such systems are also investigated experimentally like for example microwave cavities, optical cavities (microlasers) and mesoscopic devices (quantum dots).

From the numerical side, our experiences with using Python for research purposes is extremely positive. When thinking of scientific computing typically `Fortran` or `C/C++` come to ones mind first for maximum performance. However many tasks involve fairly small amounts of time-critical code, so that both development time and programm lengths are substantially reduced. On the

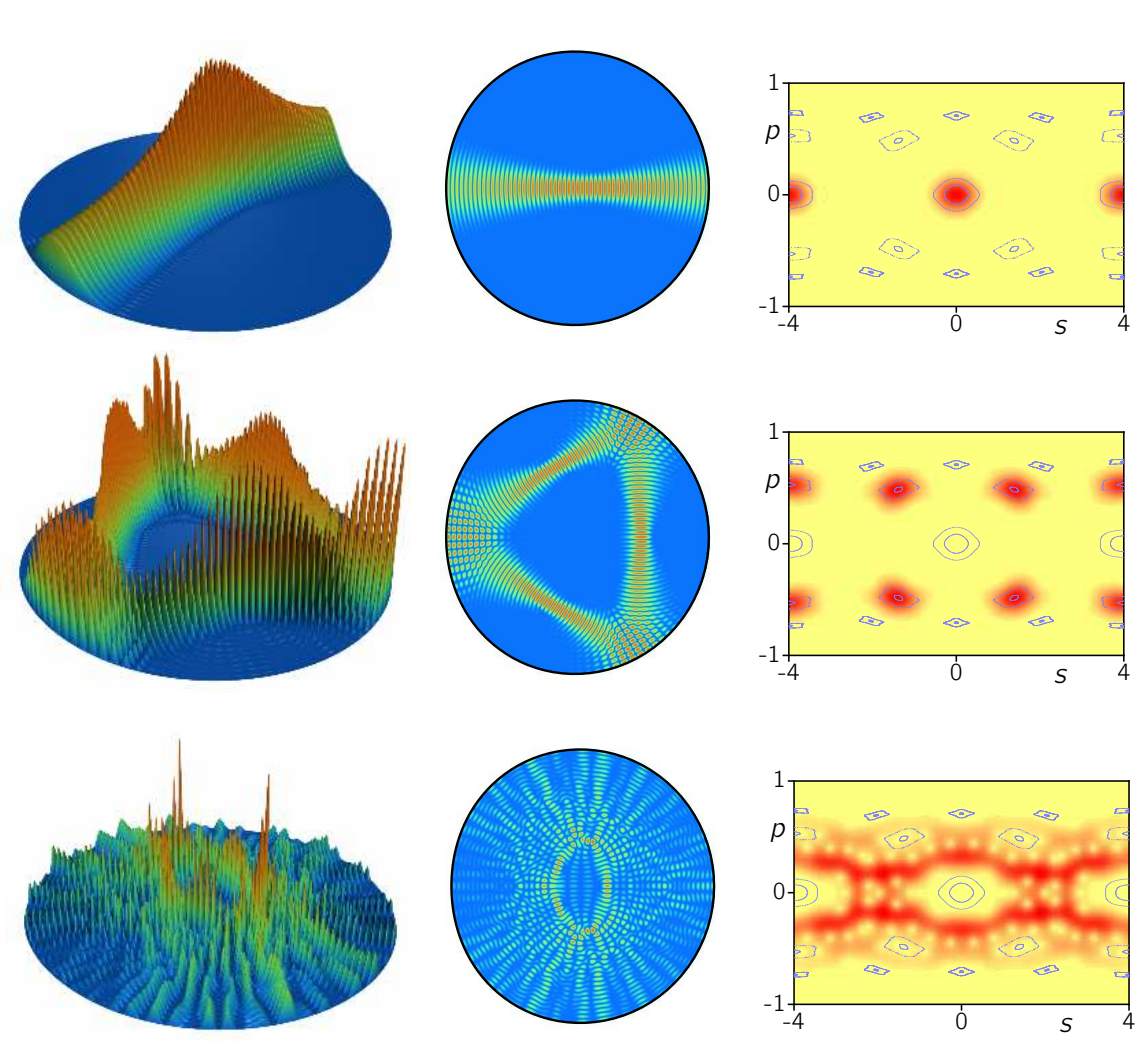

Figure 5: Eigenstates in billiard with mixed phase either concentrate in the regular islands (first two lines), or extend over the chaotic region (last line). This is most clearly seen in the quantum Poincaré Husimi representation displayed in the last column for each case.

other hand, due to the efficient usage of numerical libraries, no significant speed reduction arises in our applications.

We would also like to point out that all the illustrations shown here involve Python. For example for the two-dimensional graphics shown in Figs. 3 and 5 we have used PyX [14] (together with `PyXGraph` to simplify plotting). For the three-dimensional visualization of eigenstates `MayaVi` [15] is used with subsequent rendering.

Acknowledgements

I would like to thank L. Bittrich for useful comments on the manuscript and L. Bittrich, S. Löck, N. Hlubek and J.-M. Braun for their contributions to the `Iterator` shown in Fig. 2.

References

[1] M. Robnik: *Classical dynamics of a family of billiards with analytic boundaries*, J. Phys. A **16** (1983) 3971–3986.

[2] A. Bäcker and H. R. Dullin: *Symbolic dynamics and periodic orbits for the cardioid billiard*, J. Phys. A **30** (1997) 1991–2020.

[3] wxPython: `www.wxpython.org`.

[4] A. Bäcker and N. Hlubek: *PlottingCanvas*, see `www.physik.tu-dresden.de/~baecker`.

[5] A. Bäcker: *Numerical aspects of eigenvalue and eigenfunction computations for chaotic quantum system*, in: *The Mathematical Aspects of Quantum Maps*, M. Degli Esposti and S. Graffi (Eds.), Springer Lecture Notes in Physics **618** (2003) 91–144.

[6] R. Aurich and F. Steiner: *Statistical properties of highly excited quantum eigenstates of a strongly chaotic system*, Physica D **64** (1993) 185–214.

[7] O. Bohigas, M.-J. Giannoni and C. Schmit: *Characterization of chaotic quantum spectra and universality of level fluctuation laws*, Phys. Rev. Lett. **52** (1984) 1–4.

[8] M. V. Berry and M. Tabor: *Level clustering in the regular spectrum*, Proc. R. Soc. London Ser. A **356** (1977) 375–394.

[9] M. L. Mehta: *Random Matrices*, Academic Press, San Diego, revised and enlarged second edn., (1991).

[10] M. V. Berry: *Regular and irregular semiclassical wavefunctions*, J. Phys. A **10** (1977) 2083–2091.

[11] A. Voros: *Semi-classical ergodicity of quantum eigenstates in the Wigner representation*, in: *Stochastic Behavior in Classical and Quantum Hamiltonian Systems*, no. 93 in Lecture Notes in Physics, 326–333, Springer-Verlag, Berlin, (1979).

[12] M. V. Berry: *Semiclassical mechanics of regular and irregular motion*, in: *Comportement Chaotique des Systèmes Déterministes — Chaotic Behaviour of Deterministic Systems* (Eds. G. Iooss, R. H. G. Hellemann and R. Stora), 171–271, North-Holland, Amsterdam, (1983).

[13] A. Bäcker, R. Schubert and P. Stifter: *Rate of quantum ergodicity in Euclidean billiards*, Phys. Rev. E **57** (1998) 5425–5447.

[14] PyX: `pyx.sourceforge.net`.

[15] MayaVi: `mayavi.sourceforge.net`.